

TOWARDS IMPROVED ROOM IMPULSE RESPONSE ESTIMATION FOR SPEECH RECOGNITION

Anton Ratnarajah^{1*}, Ishwarya Ananthabhotla², Vamsi Krishna Ithapu²,
Pablo Hoffmann², Dinesh Manocha¹, Paul Calamia²

¹ University of Maryland, College Park, USA, ² Reality Labs Research at Meta, Redmond, WA USA

ABSTRACT

We propose to characterize and improve the performance of blind room impulse response (RIR) estimation systems in the context of a downstream application scenario, far-field automatic speech recognition (ASR). We first draw the connection between improved RIR estimation and improved ASR performance, as a means of evaluating neural RIR estimators. We then propose a GAN-based architecture that encodes RIR features from reverberant speech and constructs an RIR from the encoded features, and uses a novel energy decay relief loss to optimize for capturing energy-based properties of the input reverberant speech. We show that our model outperforms the state-of-the-art baselines on acoustic benchmarks (by 72% on the energy decay relief and 22% on an early-reflection energy metric), as well as in an ASR evaluation task (by 6.9% in word error rate).

Index Terms— room impulse response, blind estimation

1. INTRODUCTION

The reverberation effects in audio recordings depend on the acoustic environment (e.g., room geometry, room materials, etc.) in which they are recorded. For instance, speech in large auditoria sounds perceptually very different from speech in small meeting rooms. Such reverberation effects (i.e., early reflections, late reverberation, the amount of sound scattering and diffraction, etc.) are characterized by a transfer function known as the room impulse response (RIR). Measuring or simulating accurate RIRs for a given acoustic environment is vital for a variety of speech and audio applications including speech recognition [1, 2], speech dereverberation [3, 4], speech separation [5, 6] and augmented/virtual reality [7].

Accurate measurement of RIRs is prohibitively expensive and requires expert guidance [2]. On the other hand, simulating accurate RIRs requires 3D mesh representations of the underlying scenes [8] and complete knowledge of material properties [9, 10]. Therefore, it is not practical to precisely simulate RIRs for a real-world environment without their 3D representation. As an alternative, we propose an approach to

directly estimate the RIR from single-channel speech recordings. RIR estimation via blind system identification is a well studied problem in classical signal processing [11–13]. Recently, deep learning based end-to-end RIR estimation methods have been employed with some success [14].

In this work, we focus on an estimation framework of RIRs from the point of view of a specific use case, automatic speech recognition (ASR). It is well known that reverberant speech inputs affect the performance of ASR systems in home voice assistants, particularly in the presence of a domain mismatch between the training and test data in terms of reverberation effects [15]. Such a mismatch is a direct consequence of the need for augmenting training data similar to the test data by estimating the reverberation effects in the testing environment to ensure learnability when large neural networks are involved. In principle, one can utilize the findings from recent RIR estimation models like FiNS [14], wherein the late reverberation content is modeled via a combination of noise bases; however, we propose an alternate estimation method that explicitly leverages the goals of a speech recognizer. Additionally, while room acoustics-agnostic domain adaptation strategies have been explored to handle the domain mismatch issue [16], we draw and study an explicit connection between improved RIR estimation and improved ASR performance.

Overall, we propose an approach for speech-to-RIR estimation that directly benefits ASR. Our main contributions are twofold: We first propose a novel GAN-based RIR estimator (S2IR-GAN) using an energy decay relief loss, which we expect to capture the energy-based acoustic properties of input reverberant speech, and a discriminator loss to estimate the fine structure of the RIR. We demonstrate 22% improvement in capturing early reflection energy (ERE) and 72% improvement in energy decay relief (EDR). We then evaluate the benefits of the proposed model on an ASR task and demonstrate a 6.9% reduction of word error rate relative to existing RIR estimators when handling reverberant speech.

2. RELATED WORK

Several algorithms have been proposed to blindly estimate an RIR from a reverberant source signal using traditional signal-processing approaches [11–13, 17, 18]. For some methods

*Work done during an internship at Reality Labs Research at Meta.

that take an ℓ_1 -norm-based approach, performance depends significantly on the choice of a regularization parameter corresponding to a real-world scenario [13]; some require multi-channel speech signals [13]; and most assume that either the source signal is a modulated Gaussian pulse [17, 18], or that the speaker and microphone characteristics are known [11, 12]. For far-field ASR tasks, however, we are required to estimate RIRs from reverberant speech source signals independent of speaker and microphone characteristics.

Recently, a neural network model was proposed to estimate the RIR from single-channel reverberant speech (FiNS) [14]. The FiNS model directly estimates early RIR components, and estimates late components as a combination of decaying filtered noise signals. In contrast, we propose a GAN-based architecture (S2IR-GAN) to directly estimate the entire RIR up to 0.25 seconds. RIRs with full duration and RIRs cropped to a duration of 0.25 seconds are known to give similar performance in far-field ASR tasks in meeting rooms [19].

We explicitly train our S2IR-GAN on an energy-based cost function to estimate an RIR with a similar energy distribution as the ground-truth RIR. Estimating energy-based acoustic parameters such as reverberation time (T_{60}) and direct-to-reverberant ratio (DRR) and incorporating them in speech dereverberation and speech recognition systems have shown improved performance [20–22]. Therefore, we expect that accurately estimating the energy distribution in the estimated RIRs helps the S2IR-GAN model improve its performance over other approaches in far-field ASR tasks.

3. OUR APPROACH

3.1. RIR Estimation from Reverberant Speech

We alternatively train our RIR estimation network (E_N) and a discriminator network (D_N) using reverberant speech (S_R) and the corresponding RIR (R_G) in the data distribution p_d at each iteration. Our RIR estimation network estimates the RIR of the input reverberant speech and our discriminator network is optimized to differentiate the estimated RIR from the ground truth RIR. The objective function of E_N consists of the EDR error (see below), the modified conditional GAN (CGAN) [19] error, and the mean square error (MSE). We use a modified CGAN objective function to train D_N .

EDR Error: The EDR describes the energy remaining in the RIR in a specific frequency band centered at b_k Hz at time t seconds. In the following EDR equation, $H(r, t, k)$ is the bin k of the short-time Fourier transform of the RIR r at time t . The total number of time frames is T .

$$EDR(r, t, b_k) = \sum_{t=t}^T |H(r, t, k)|^2. \quad (1)$$

We calculate the EDR of the estimated RIR (R_E) and the ground truth RIR (R_G) at a set of octave frequency bands (B) with center frequencies from 16Hz to 4000 Hz. We calculate

the EDR loss as follows:

$$\mathcal{L}_{EDR} = \mathbb{E}_{(S, R_G) \sim p_d} [\mathbb{E}[(EDR(R_E, t, b_k) - EDR(R_G, t, b_k))^2]]. \quad (2)$$

Our EDR loss helps the RIR estimator to capture energy-based acoustic properties of the RIR [23].

CGAN Error (RIR Estimator): The CGAN error is used to estimate the RIR from the reverberant speech (S_R) using our RIR estimator (E_N) that is difficult to differentiate from the ground truth RIR by the D_n during training.

$$\mathcal{L}_{CGAN} = \mathbb{E}_{S_R \sim p_d} [\log(1 - D_N(E_N(S_R)))]. \quad (3)$$

MSE: For each reverberant speech example (S_R), we calculate the squared difference of each time sample (t) in the estimated RIR R_E and the ground truth RIR R_G .

$$\mathcal{L}_{MSE} = \mathbb{E}_{(S_R, R_G) \sim p_d} [\mathbb{E}[(R_G(S_R, t) - R_E(S_R, t))^2]]. \quad (4)$$

We alternatively train E_N to minimize the objective function \mathcal{L}_{E_N} and D_N to maximize the objective function \mathcal{L}_{D_N} . We use the weights λ_{EDR} and λ_{MSE} to control the contribution of \mathcal{L}_{EDR} and \mathcal{L}_{MSE} respectively in \mathcal{L}_{E_N} :

$$\mathcal{L}_{E_N} = \mathcal{L}_{CGAN} + \lambda_{EDR} \mathcal{L}_{EDR} + \lambda_{MSE} \mathcal{L}_{MSE}, \quad (5)$$

$$\mathcal{L}_{D_N} = \mathbb{E}_{(R_G, S_R) \sim p_d} [\log(D_N(R_G(S_R)))] + \mathbb{E}_{S_R \sim p_d} [\log(1 - D_N(E_N(S_R)))]. \quad (6)$$

3.2. Network Architecture

RIR Estimator: We propose an encoder-decoder architecture to estimate the RIR from the reverberant speech (Fig. 1). The reverberant speech (S_R) can be described as a convolution of clean speech (S_C) and an RIR as follows:

$$S_R[n] = \sum_{s=1}^S RIR[s] * S_C[n - s], \quad (7)$$

where S is the total number of samples in the RIR. To capture the features of the RIR of length 4096 from the reverberant speech, we use a large convolutional layer of length 8193 in the first layer. Later, we reduce the dimension of the extracted RIR features from 64 to 16 while increasing the number of channels from 512 to 1024.

We construct the RIR from the encoded features in the decoder network. We use 5 sets of transpose convolution layers, batch normalization and PReLU layers to gradually increase the length from 16 to 4096 and reduce the number of channels from 1024 to 64. We use a transpose convolution layer with stride 1 to collapse the number of channels from 64 to 1 and obtain the weighted averaged estimated RIR. In the last layer, we use the Tanh activation function because the RIR contains both negative and positive values. Fig. 1 shows our encoder-decoder architecture in detail. We adapt the discriminator (D_N) network architecture from FAST-RIR [19].

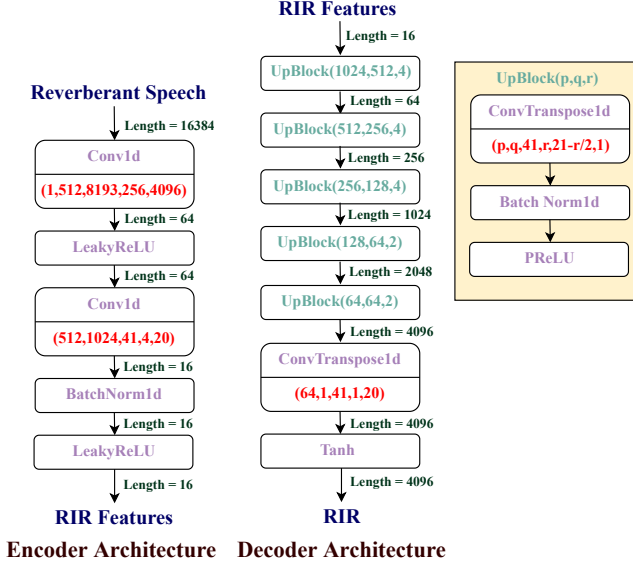


Fig. 1: The encoder-decoder architecture of our S2IR-GAN. Our encoder network extracts the RIR features, and our decoder network constructs an RIR from the extracted features. For Conv1d layers and ConvTranspose1d layers, the parameters are input channels, output channels, kernel size, stride and padding. The last parameter of ConvTranspose1d is output padding. We use a negative slope of 0.2 for the Leaky ReLU layers.

3.3. Dataset and Training

We generate 98,316 one-second duration synthetic training examples of reverberant speech by convolving 360 hours of clean speech (train-clean-360) from the LibriSpeech dataset [24] with RIRs from the Meta RIR (MRIR) dataset. To pick the best model during training, we use the validation EDR loss. We trained our network for 200 epochs using the RMSprop optimizer. We used a batch size of 128 and an initial learning rate of 8×10^{-5} . The learning rate is decayed by 0.7 after every 40 epochs.

4. ACOUSTIC EVALUATION

We evaluate the performance of our proposed approach using EDR loss (Equation 2), DRR error, early reflection energy (ERE) loss and MSE (Equation 4) of the estimated RIR and the ground truth RIR. Finally, we also compare the ground truth RIR and the estimated RIR using our S2IR-GAN in the time domain.

The EDR of the RIR contains enough information to construct an equivalent RIR with the same gross temporal and spectral features while the fine structure can be different [25]. Acoustic parameters such as T_{60} and early decay time are measured on the slope of EDR. Therefore, we use EDR loss for evaluation. DRR, the log ratio of the energy of the direct sound and the sound arriving after it, is an acoustic parameter

often used in ASR applications to measure the amount of distortion introduced into speech by the RIR [26]; DRR estimation is also directly integrated into some ASR systems [21]. Here, we compute the DRR error as the mean absolute error (MAE) of the DRR between the estimated and the ground-truth RIRs. We also include the ERE loss, which is the MAE of the early reflection energy between the estimated and the ground truth RIR. ERE measures the total early sound energy between 0 and 80ms:

$$ERE = 10 \log \text{Energy}(0 - 80ms). \quad (8)$$

We created 5000 reverberant test data by convolving clean speech from the LibriSpeech dataset (train-clean-100) with RIRs from the MRIR dataset not used for training. We compared our performance against a baseline model and the state-of-the-art RIR estimator (FiNS). We modified the input and output dimensions of the FiNS model to match our S2IR-GAN. For a fair comparison, we have trained FiNS and our S2IR-GAN using the same training data (Section 3.3). We use a pre-trained open-source speech enhancement toolkit named ESPNET-SE [27] as a baseline model.

Baseline: ESPNET-SE can perform speech dereverberation and denoising. We pass the reverberant speech test data as the input to the network and get clean speech as the output. We compute the RIR using the reverberant speech (S_R) and the corresponding output clean speech (S_C) as follows:

$$RIR = \mathcal{F}^{-1} \left(\frac{\mathcal{F}(S_R)}{\mathcal{F}(S_C)} \right), \quad (9)$$

where \mathcal{F} and \mathcal{F}^{-1} are the Fourier transform and inverse Fourier transform, respectively.

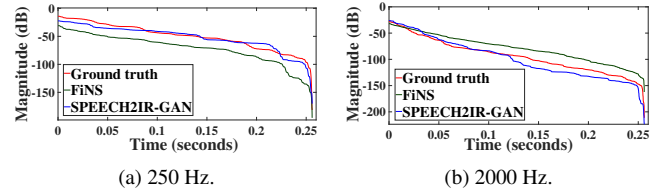


Fig. 2: The EDR (Equation 1) of the ground truth RIR, and the estimated RIR using FiNS and our S2IR-GAN models at 250 HZ and 2000 Hz. We can see that the EDR of S2IR-GAN is closest to the ground truth EDR.

Table 1 shows the EDR loss and ERE loss for the baseline model, FiNS and our S2IR-GAN. We calculate the loss over the octave-bands with center frequencies up to 4000 Hz. We can see that on average, our proposed S2IR-GAN outperforms the FiNS by 72% in EDR loss and 22% in ERE loss. In Fig. 2, we can see the ground truth EDR and the EDR of the estimated RIRs using FiNS and S2IR-GAN at 250 Hz and 2000 Hz. The EDR of our S2IR-GAN is closest to the ground truth EDR.

We calculated the MSE and DRR error of the estimated RIRs for 3 different methods (Table 2). We can see that Base-

Table 1: Energy decay relief (EDR) loss (Equation 2) and the mean absolute error of the early reflection energy (ERE loss). In this table, we compare the baseline model, FiNS [14] and our proposed S2IR-GAN. The best results are shown in **bold**.

Loss Method	Frequency								
	16Hz	32Hz	63Hz	125Hz	250Hz	500Hz	1000Hz	2000Hz	4000Hz
EDR Loss Baseline	8.3×10^{-1}	1.7×10^{-5}	4.4×10^{-6}	7.7×10^{-5}	2.2×10^{-3}	1.4×10^{-3}	8.4×10^{-2}	1.6×10^{-3}	1.0×10^{-1}
FiNS	7.9×10^{-10}	1.6×10^{-10}	4.6×10^{-10}	6.8×10^{-5}	1.0×10^{-3}	2.3×10^{-4}	6.9×10^{-4}	1.0×10^{-3}	3.3×10^{-2}
Ours	1.8×10^{-11}	1.9×10^{-11}	3.4×10^{-10}	2.0×10^{-5}	3.8×10^{-4}	5.9×10^{-5}	1.4×10^{-4}	2.2×10^{-4}	8.3×10^{-3}
ERE Loss Baseline	8.75	7.66	4.47	13.31	11.41	6.44	5.65	7.67	5.80
FiNS	7.41	6.89	4.69	3.77	4.21	3.62	3.81	3.75	3.67
Ours	5.88	5.33	3.34	3.27	3.11	2.88	2.87	2.83	2.91

Table 2: MSE (Equation 4) and DRR error of the estimated RIRs from the baseline model, FiNS [14] and S2IR-GAN.

METHOD	MSE	DRR (dB)
Baseline	3.0×10^{-4}	6.63
FiNS	3.7×10^{-4}	3.31
S2IR-GAN (ours)	3.0×10^{-4}	3.28

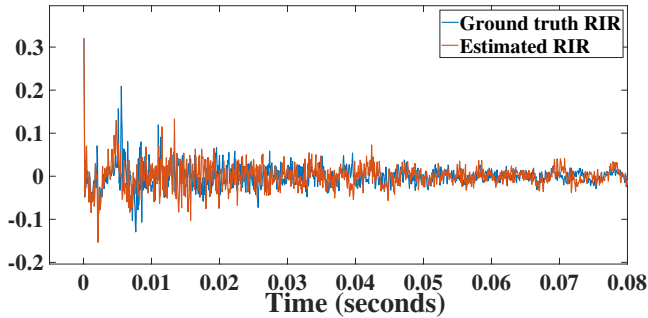


Fig. 3: Time domain plot of the ground truth RIR and the estimated RIR from our S2IR-GAN. The estimated RIR has similar macroscopic structure as the ground truth RIR while the fine structure differs from the ground truth RIR.

line and S2IR-GAN give the lowest MSE error. Baseline gives higher DRR error when compared to S2IR-GAN. Fig. 3 shows an example of the ground truth RIR and the estimated RIR from our S2IR-GAN. We can see that our network can estimate general patterns in the ground truth RIR. However, our network cannot accurately estimate the fine temporal structure of the ground truth RIR. The estimated RIRs are perceptually similar to the ground truth RIR, as can be heard through audio samples of ground truth RIRs and estimated RIRs¹.

5. ASR EVALUATION

We evaluate the performance of our S2IR-GAN in the Kaldi automatic speech recognition (ASR) experiment². We use close-talk speech data (IHM) and far-field speech data (SDM) in the AMI corpus [28] for our experiment. From the SDM corpus, we sample 2000 reverberant speech examples of ap-

¹<https://anton-jeran.github.io/S2IR/>

²<https://github.com/RoyJames/kaldi-reverb/>

Table 3: Far-field ASR results were obtained for far-field speech data recorded by single distance microphones (SDM) in the AMI corpus. The best results are shown in **bold**.

Training Dataset Clean Speech ⊗ RIR	Word Error Rate [%]
IHM ⊗ None	64.2
IHM ⊗ FiNS	60.9
IHM ⊗ S2IR-GAN (ours)	54.0

proximately one second duration. We input the sampled reverberant speech to the FiNS model and our proposed S2IR-GAN and estimate the RIRs from the input speech. The anechoic IHM speech is convolved with the estimated RIRs to create synthetic reverberant speech training data.

We train the modified Kaldi ASR recipe with the synthetic training data and test the ASR model on the real-world reverberant SDM data. We also train the ASR model with unmodified IHM data as our baseline model. We use word error rate (WER) to evaluate the performance of the ASR system. Lower WER indicates that the reverberation effects in the training speech data are closer to the test speech data (SDM) [10]. From Table 3, we can see that our S2IR-GAN outperforms FiNS by 6.9%.

6. DISCUSSION

In this work, we present a method for the improved estimation of RIRs in the context of far-field speech recognition. Our S2IR-GAN model outperforms the state-of-the-art RIR estimator (FiNS) in acoustic metrics such as energy decay relief loss, early reflection energy loss, DRR error, and MSE. It is also shown to outperform FiNS in a downstream ASR task. The main limitation of this work is that the network cannot capture the fine temporal structure of an RIR from reverberant speech, though the perceptual implications of this shortcoming are unclear. In the future, we would like to extend this work to improve performance of the current model by expanding the set of RIRs used to augment training data; consider RIR estimation while leveraging the goals of other downstream tasks such as dereverberation or source separation; or estimate RIRs from a larger set of input modalities, such as multi-channel speech signals or audio-visual data.

7. REFERENCES

- [1] Anton Ratnarajah, Zhenyu Tang, and Dinesh Manocha, “IR-GAN: room impulse response generator for far-field speech recognition,” in *Interspeech*. 2021, pp. 286–290, ISCA.
- [2] Igor Szöke, Miroslav Skácel, Ladislav Mosner, Jakub Paliesek, and Jan Honza Cernocký, “Building and evaluation of a real room impulse response dataset,” *IEEE J. Sel. Top. Signal Process.*, vol. 13, no. 4, pp. 863–876, 2019.
- [3] Yi Luo and Jianwei Yu, “Fra-rir: Fast random approximation of the image-source method,” *ArXiv*, vol. abs/2208.04101, 2022.
- [4] Yan Zhao, DeLiang Wang, Buye Xu, and Tao Zhang, “Monaural speech dereverberation using temporal convolutional networks with self attention,” *IEEE ACM Trans. Audio Speech Lang. Process.*, vol. 28, pp. 1598–1607, 2020.
- [5] Rohith Aralikatti et al., “Improving reverberant speech separation with synthetic room impulse responses,” in *ASRU*. 2021, pp. 900–906, IEEE.
- [6] Teerapat Jenrungrot, Vivek Jayaram, Steven M. Seitz, and Ira Kemelmacher-Shlizerman, “The cone of silence: Speech separation by localization,” in *NeurIPS*, 2020.
- [7] Carl Schissler, Ravish Mehra, and Dinesh Manocha, “High-order diffraction and diffuse reflections for interactive sound propagation in large environments,” *ACM Trans. Graph.*, vol. 33, no. 4, jul 2014.
- [8] Anton Ratnarajah et al., “Mesh2ir: Neural acoustic impulse response generator for complex 3d scenes,” in *Proceedings of the 30th ACM International Conference on Multimedia*, New York, NY, USA, 2022, MM ’22, p. 924–933, Association for Computing Machinery.
- [9] Changan Chen, Carl Schissler, Sanchit Garg, Philip Kobernik, Alexander Clegg, Paul Calamia, Dhruv Batra, Philip W Robinson, and Kristen Grauman, “Soundspaces 2.0: A simulation platform for visual-acoustic learning,” *arXiv*, 2022.
- [10] Zhenyu Tang et al., “Gwa: A large high-quality acoustic dataset for audio processing,” in *ACM SIGGRAPH 2022 Conference Proceedings*, New York, NY, USA, 2022, SIGGRAPH ’22, Association for Computing Machinery.
- [11] Yuanqing Lin and Daniel D Lee, “Bayesian regularization and nonnegative deconvolution for room impulse response estimation,” *IEEE Transactions on Signal Processing*, vol. 54, no. 3, pp. 839–847, 2006.
- [12] Koby Crammer and Daniel D Lee, “Room impulse response estimation using sparse online prediction and absolute loss,” in *2006 IEEE International Conference on Acoustics Speech and Signal Processing Proceedings*, 2006, vol. 3, pp. III–III.
- [13] Marco Crocco and Alessio Del Bue, “Room impulse response estimation by iterative weighted L_1 -norm,” in *2015 23rd European Signal Processing Conference (EUSIPCO)*, 2015, pp. 1895–1899.
- [14] Christian J. Steinmetz, Vamsi Krishna Ithapu, and Paul Calamia, “Filtered noise shaping for time domain room impulse response estimation from reverberant speech,” in *WASPAA*. 2021, pp. 221–225, IEEE.
- [15] Dong Yu and Jinyu Li, “Recent progresses in deep learning based acoustic models,” *IEEE CAA J. Autom. Sinica*, vol. 4, no. 3, pp. 396–409, 2017.
- [16] Hank Liao, “Speaker adaptation of context dependent deep neural networks,” in *2013 IEEE International Conference on Acoustics, Speech and Signal Processing*, 2013, pp. 7947–7951.
- [17] Maozhong Fu, Jesper Rindom Jensen, Yuhuan Li, and Mads Græsbøll Christensen, “Sparse modeling of the early part of noisy room impulse responses with sparse bayesian learning,” in *ICASSP 2022 - 2022 IEEE International Conference on Acoustics, Speech and Signal Processing (ICASSP)*, 2022, pp. 586–590.
- [18] Matti Karjalainen, Poju Ansalo, Aki Mäkitvirta, Timo Peltonen, and Vesa Välimäki, “Estimation of modal decay parameters from noisy response measurements,” *Journal of the Audio Engineering Society*, vol. 50, no. 11, pp. 867–878, november 2002.
- [19] Anton Ratnarajah, Shi-Xiong Zhang, Meng Yu, Zhenyu Tang, Dinesh Manocha, and Dong Yu, “Fast-rir: Fast neural diffuse room impulse response generator,” in *ICASSP*. 2022, pp. 571–575, IEEE.
- [20] Bo Wu, Kehuang Li, Minglei Yang, and Chin-Hui Lee, “A reverberation-time-aware approach to speech dereverberation based on deep neural networks,” *IEEE/ACM Transactions on Audio, Speech, and Language Processing*, vol. 25, no. 1, pp. 102–111, 2017.
- [21] Ritwik Giri, Michael L. Seltzer, Jasha Droppo, and Dong Yu, “Improving speech recognition in reverberation using a room-aware deep neural network and multi-task learning,” in *2015 IEEE International Conference on Acoustics, Speech and Signal Processing (ICASSP)*, 2015, pp. 5014–5018.
- [22] Helin Wang, Bo Wu, Lianwu Chen, Meng Yu, Jianwei Yu, Yong Xu, Shi-Xiong Zhang, Chao Weng, Dan Su, and Dong Yu, “Tecanet: Temporal-contextual attention network for environment-aware speech dereverberation,” in *Interspeech*. 2021, pp. 1109–1113, ISCA.
- [23] Sagnik Majumder, Changan Chen, Ziad Al-Halah, and Kristen Grauman, “Few-shot audio-visual learning of environment acoustics,” *ArXiv*, vol. abs/2206.04006, 2022.
- [24] Vassil Panayotov, Guoguo Chen, Daniel Povey, and Sanjeev Khudanpur, “Librispeech: An ASR corpus based on public domain audio books,” in *ICASSP*. 2015, pp. 5206–5210, IEEE.
- [25] M. R. Schroeder, “New method of measuring reverberation time,” *The Journal of the Acoustical Society of America*, vol. 37, no. 6, pp. 1187–1188, 1965.
- [26] Alessio Brutti and Marco Matassoni, “On the use of early-to-late reverberation ratio for asr in reverberant environments,” in *2014 IEEE International Conference on Acoustics, Speech and Signal Processing (ICASSP)*, 2014, pp. 4638–4642.
- [27] Chenda et al., “Espnet-se: End-to-end speech enhancement and separation toolkit designed for asr integration,” in *2021 IEEE Spoken Language Technology Workshop (SLT)*, 2021, pp. 785–792.
- [28] J Carletta et al., “The AMI meeting corpus: A pre-announcement,” in *Proceedings of the Second International Conference on Machine Learning for Multimodal Interaction*. 2005, MLMI’05, p. 28–39, Springer-Verlag.